

# Recent Progress in Fiber Fabrication Techniques by Vapor-Phase Axial Deposition

KOICHI INADA, MEMBER, IEEE

(Invited Paper)

**Abstract**—Five years have passed since the invention of the VAD technique. Fabrication techniques for the various kinds of VAD fibers such as graded index fibers, single-mode fibers, high NA fibers, and single polarization fibers have been developed. This paper mainly outlines the recent improvements in the VAD fiber manufacturing techniques such as the preform fabrication technique, dehydration technique, refractive index profile formation technique, and the single-mode fiber manufacturing technique.

## I. INTRODUCTION

THE vapor-phase axial deposition technique (VAD) was developed at Ibaraki Electrical Communication Laboratory, NTT, and reported at the First IOOC Conference held in Tokyo in 1977 [1]. The transmission loss reported at the conference was 5 dB/km. However, much attention was payed from the mass production and economical points of view because the VAD process had the possibility of continuous fabrication of high silica fiber preforms and the deposition speed was extremely fast compared to that of the MCVD process.

Now, five years have passed since the invention of the VAD technique. Fabrication techniques for the various kinds of VAD fibers such as graded index fibers, single-mode fibers, high NA fibers, and single polarization fibers have been developed and improved. The fiber preform fabrication technique by the VAD method has been reported by Izawa and Inagaki in [2]. After that, VAD fibers have been manufactured on a mass production scale. The graded index VAD fibers have been installed for the second field trial in Kawasaki in 1980 [3] and for the commercial test in several places in Japan in 1981.

VAD soot preforms have a high OH content because the soot is formed in an oxy-hydrogen flame. Several dehydration techniques have been developed, and in 1980, ultimately low OH content fiber was achieved, whose OH absorption loss at 1.39  $\mu\text{m}$  was only 0.04 dB/km, and the residual OH content was estimated at less than 1 ppb [4], [5].

This paper mainly outlines the recent improvements in the VAD fiber manufacturing techniques such as the preform fabrication technique, dehydration technique, refractive index profile formation technique, and the single-mode fiber manufacturing technique.

Manuscript received April 1, 1982; revised May 24, 1982.  
The author is with Fujikura Cable Works, Ltd., Chiba-ken, Japan.

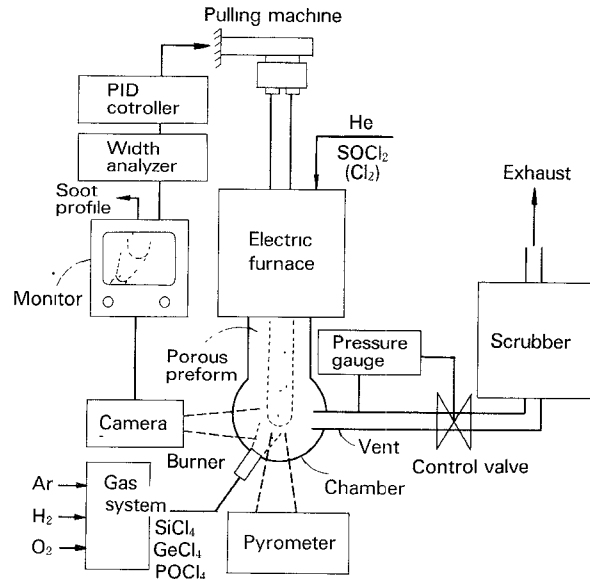


Fig. 1. Schematic diagram of VAD apparatus.

## II. PREFORM FABRICATION

The VAD preform fabrication technique has been much improved in the last several years. A typical apparatus for the VAD preform fabrication is shown in Fig. 1 [6]. Fine glass particles synthesized in the oxy-hydrogen flame are deposited onto the end surface of the seed rod which is usually made of silica. A porous preform is then grown along the axial direction. The end position of the porous preform is constantly regulated by monitoring it with an ITV camera for a uniform growth of the preform.

One of the advantages of the VAD technique is the high deposition speed. The speed is mainly determined by the burner configuration, gas flow conditions, chamber construction, and the size of the consolidation furnace. It must be increased while keeping a good graded index profile. The porous preform is then dehydrated and consolidated into a transparent preform in a graphite furnace at a temperature of about 1500°C.

The typical process parameters are listed in Table I [7]–[17]. The maximum deposition speed of 2.0 g/min was achieved, although the refractive index profile and the deposition efficiency are somewhat degraded [7]. The as-grown transparent preform

TABLE I  
TYPICAL PROCESS PARAMETERS AND THE TOP DATA

Deposition speed	2.0 gr/min [7], 0.5-1.7 gr/min [8]
Deposition efficiency	60-80 percent [8]
Diameter (as-grown)	
Porous preform	58 mm x 350 mm [9], 60 mm [10]-[12] 70 mm [8], 52 mm x 300 mm [13]
Transparent preform	23 mm [10], [13], 24 mm [9] 25 mm [11], [12], [8], 30 mm [14]
Continuous fiber length	100 km [14], 21 km [15], [16], 30 km [17]

is elongated in an oxy-hydrogen flame with a glass lathe and put into a thick wall silica tube by a rod-in-tube method. Table II shows the typical VAD process [18].

The VAD process has a high deposition speed and a large preform size. However, it has several accompanying processes such as the dehydration process, consolidation process, elongation process, and the rod-in-tube process. These processes make the total process time long. In order to reduce the long process time, a continuous process of soot preform deposition and consolidation into a transparent glass preform was developed [19] and a large size preform, which corresponds to 100 km in fiber length, has been fabricated [20]. The apparatus used was essentially the same as in Fig. 1.

In the continuous consolidation process, the pulling speed of the consolidated preform must be matched with the relation among the soot preform growing speed, shrinkage rate of the soot preform in the axial direction, and the elongation rate of the transparent preform at the necking down position, which is the function of the weight of soot preform, bulk density of soot preform, dopant content, and sintering temperature.

Materials used in the VAD method are basically the same as those used in the MCVD method.  $\text{GeO}_2$  is doped for the refractive index profile formation. A small amount of  $\text{P}_2\text{O}_5$  is doped so as to reduce the Rayleigh scattering loss.

Germanium is one of the rare materials and the cost for  $\text{GeO}_2$  is estimated to share a large part for the material cost of high silica fibers. However, other oxide materials like  $\text{PbO}$ ,  $\text{CaO}$ , and  $\text{BaO}$ , which are common on the earth, have been difficult to dope into silica glass by the MCVD method or the VAD method. It is possible to dope these materials by carrying the dopant material in a liquid phase with a small modification of the VAD process.  $\text{PbO}$  was doped by using a  $\text{Pb}(\text{NO}_3)_2$  water solution [21]. The refractive index increase by doping  $\text{PbO}$  was about 0.8 percent. The losses at 0.85 and 1.06  $\mu\text{m}$  were 3.3 and 2.3 dB/km, respectively.

### III. DEHYDRATION

VAD fibers fabricated without dehydration treatment usually contain high OH concentrations of about 5-30 ppm. This is because of the OH-ion contamination directly from the oxy-hydrogen flame.

In 1978, the OH content in the VAD fiber was reduced to about 0.4 ppm utilizing the chemical reaction of the  $\text{SOCl}_2$  with OH ions and  $\text{H}_2\text{O}$  molecules in the porous glass rod [22].

TABLE II  
TYPICAL VAD PROCESSES

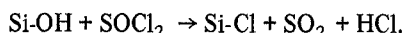
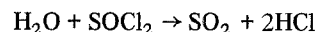
Soot preform	deposition of fine glass particles by flame hydrolysis reaction
Dehydration treatment and sintering	Dehydration by $\text{Cl}_2$ or $\text{SOCl}_2$ at about 1200 °C then sintered at about 1500 °C. The rod diameter after the sintering is about 25 mm.
Preform elongation	In an oxy-hydrogen flame, elongated rod diameter is about 10 mm.
Jacketing	Thick wall silica tube with rod-in-tube method.

In 1979, further progress in the dehydration of VAD fiber was achieved by increasing the  $\text{SOCl}_2$  treatment temperature [23]. The OH content in these fibers was around 0.05 ppm with a lowest value of 0.03 ppm. This is comparable to the level attained with the MCVD method.

From the viewpoint of optical fiber mass fabrication, it is desirable to dehydrate the soot preforms simultaneously with the consolidation process. This technique has been developed using a specially designed muffle-type resistance furnace [24] as shown in Fig. 2.

In 1980, ultimately low OH content optical fibers were developed by optimizing the dehydration process [4], [5]. The OH absorption loss increase at 1.39  $\mu\text{m}$  was only 0.04 dB/km, and the residual OH content was estimated at less than 1 ppb. Fig. 3 shows the progress of loss spectrum in each stage of the development of the above dehydration techniques [25].

$\text{SOCl}_2$  vapor in oxygen gas [22]-[24], [26] or chlorine gas [4] is used for the dehydration process. Active Cl ions produced by the thermal decomposition of  $\text{SOCl}_2$  react with OH ions and  $\text{H}_2\text{O}$  molecules in the following manner [22]:



In the reaction, there are two critical temperatures of 700 and 1200 °C as shown in Fig. 4 [23]. This is limited by the chemical reaction between OH ions and  $\text{SOCl}_2$  on the particle surfaces rather than OH diffusion because the OH diffusion length in silica glass during the dehydration time is about 5.5  $\mu\text{m}$  at 600 °C, which is larger than the particle size [26]. The residual OH concentration is also a function of the  $\text{SOCl}_2$  flow rate. The larger the flow rate, the smaller the residual OH content [26]. As a result, a dehydration temperature above 1200 °C is necessary to reduce the OH content to below 0.1 ppm.

OH contamination in the fiber core is derived from two main origins, namely insufficient dehydration of the porous preform and diffusion from both the preform outer surface during the elongation process and from the jacketing silica tube. A thin part of the elongated preform outer layer and silica jacketing tube contains OH ions at a concentration as high as 200 ppm, much higher than in the dehydrated and consolidated preform. Therefore, a thick cladding layer of about 7-10  $\mu\text{m}$  in fiber is

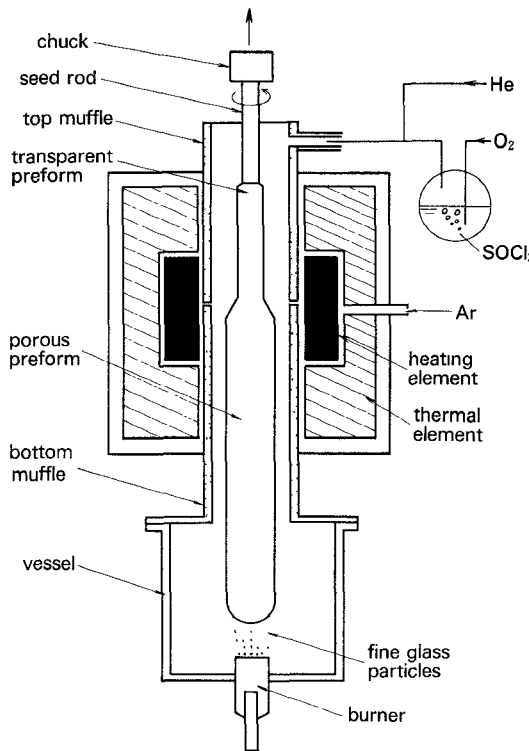


Fig. 2. Muffle-type electric furnace for consolidation simultaneously with dehydration in  $\text{SOCl}_2$  atmosphere.

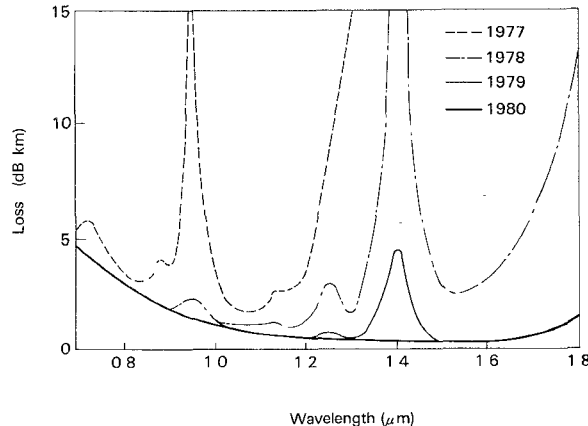


Fig. 3. Progress of transmission loss of graded index VAD fiber in each stage of the development.

needed to avoid the OH contamination from silica tube and preform surface [4], [5]. The estimated diffusion length of the OH ions into the synthesized silica glass is about 5-10  $\mu\text{m}$  under actual drawing conditions [27].

The dehydration process in the VAD method is an extra process compared with the MCVD method. However, if the dehydration treatment is completely done and if the cladding layer is sufficiently thick, the loss increase due to the OH ions is extremely small.

In the MCVD method, fibers have usually been fabricated from 99.9999 percent pure raw materials in order to avoid the loss increase due to OH ions which mainly come from  $\text{SiHCl}_3$ . On the other hand, the VAD method can use low-grade  $\text{SiCl}_4$

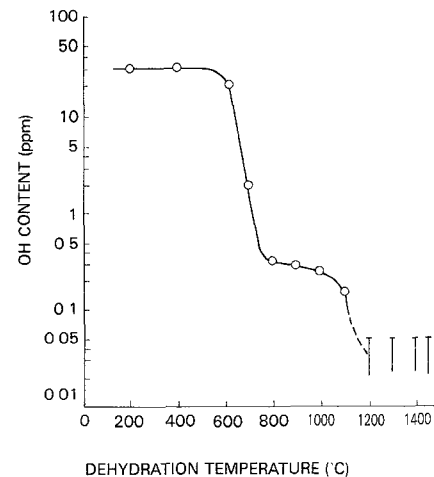


Fig. 4. OH-content versus the dehydration temperature.

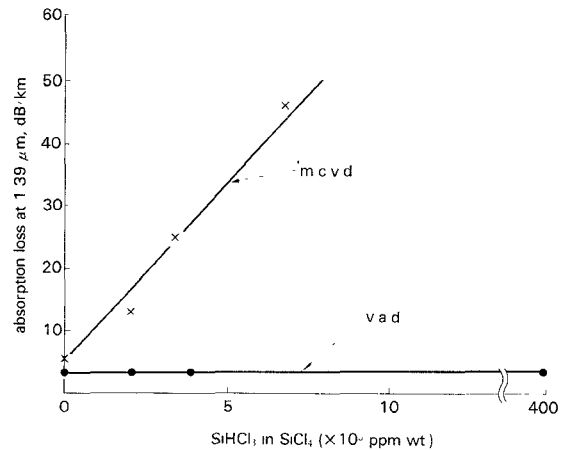


Fig. 5. Relationship between the amount of  $\text{SiHCl}_3$  in raw materials and fiber absorption loss at  $1.39 \mu\text{m}$ .

so far as the dehydration treatment is performed [28]. Fig. 5 shows the relation between the loss peaks at  $1.39 \mu\text{m}$  in the VAD fibers and the amount of impurity  $\text{SiHCl}_3$  in  $\text{SiCl}_4$ , together with the data on MCVD fibers [28]. In the case of MCVD fibers, the loss peaks increase linearly. On the other hand, the OH contamination levels in VAD fibers are constant even for 40 percent by weight added  $\text{SiHCl}_3$  in  $\text{SiCl}_4$ .

#### IV. FORMATION MECHANISM OF REFRACTIVE INDEX PROFILE

In the early stage of development, it was considered difficult to make a good graded index fiber by the VAD method. However, many techniques of controlling the refractive index profile have been developed by studying the refractive index profile formation mechanism [10], [16], [17], [29]-[31].

The profile formation mechanism in the VAD method is not simple. Much data have been accumulated about the refractive index profiles and many factors that control the fiber profile such as burner configuration, position of burner, flow rates of several raw materials, shape of soot preform, and the temperature of the surface of soot have been studied. Very small changes of these conditions change the profile substantially.

However, after getting the best conditions, if the repeatability is good, the VAD method can make constantly wide bandwidth fibers. It was fortunate that there existed some conditions that could make a wide band graded index fiber.

Basically, the dopant concentration profile in a porous preform is different from the refractive index profile in a consolidated preform because the soot density is not constant for the radius. The density is normally higher in the center than in the surroundings [32]. Moreover, crystalline phase  $\text{GeO}_2$ , which is formed in a lower temperature than  $400^\circ\text{C}$ , sublimated during the consolidation process [33], [34].

The glassy  $\text{GeO}_2$  whose concentration linearly increases when the surface temperature increases from  $500$ – $700^\circ\text{C}$ , as shown in Fig. 6 [34], determines the refractive index profile. Therefore, the surface temperature of the porous preform is one of the most important factors to control the refractive index profile. Fig. 7 shows the refractive index profile obtained when the porous soot preform was made by changing the  $\text{H}_2$  flow rate, that is, the flame temperature of the oxy-hydrogen burner was changed. When the  $\text{H}_2$  flow rate is increased, the flame temperature rose and the coefficient of refractive index profile  $\alpha$  is increased. The amount of doped  $\text{GeO}_2$  is a function of both surface temperature and  $\text{H}_2$  flow rate. Fig. 8 shows the experimentally obtained deposition properties of  $\text{GeO}_2$  [31]. As the surface temperature increases under the constant  $\text{H}_2$  flow rate, the noncrystalline  $\text{GeO}_2$  increases.

The surface temperature of the porous preform is the function of 1) the flame temperature of the oxygen-hydrogen burner, 2) the location of burner to the soot preform, 3) the shape of soot preform, and so on. Moreover, soot density and deposition efficiency are also the functions of the above factors.

In addition to the above temperature effect, if the burner has multilayers and the flow rates of  $\text{GeCl}_4$  to  $\text{SiCl}_4$  between the center layer and second layer are changed, the refractive index profile will be changed due to the dispersion effect of the dopant [35]. For example, Fig. 9 shows the change of the refractive index profiles when the flow ratio ( $R$ ) of  $\text{SiCl}_4$  which spouts from the second layer to the mixed gas of  $\text{SiCl}_4$ ,  $\text{GeCl}_4$ , and  $\text{POCl}_3$ , which spouts from the center layer, is changed. In this experiment, the maximum surface temperature of the soot rod is kept constant at  $650^\circ\text{C}$ .

The value of  $\alpha$  can be also changed by controlling the amount of  $\text{H}_2$  and  $\text{Cl}_2$  gases spout out of the burner [30]. Fig. 10 shows the changes of refractive index profiles against the four different partial pressures of  $\text{H}_2$  and  $\text{Cl}_2$  gases. In this case, when the amount of  $\text{H}_2$  and  $\text{Cl}_2$  increase, the value of  $\Delta n$  becomes smaller and the value of  $\alpha$  becomes closer to 2.

As mentioned above, reproducibility is especially important in the VAD method. The reproducibility can be monitored by measuring the surface temperature distribution of the porous soot preform.

Fig. 11 shows the computer aided on-line monitoring device on refractive index distribution [31]. The refractive index profile cannot be directly measured even if the relation between surface temperature and noncrystalline  $\text{GeO}_2$  concentration is known because the radial density of the porous preform is not constant. However, much experimentally obtained data on the

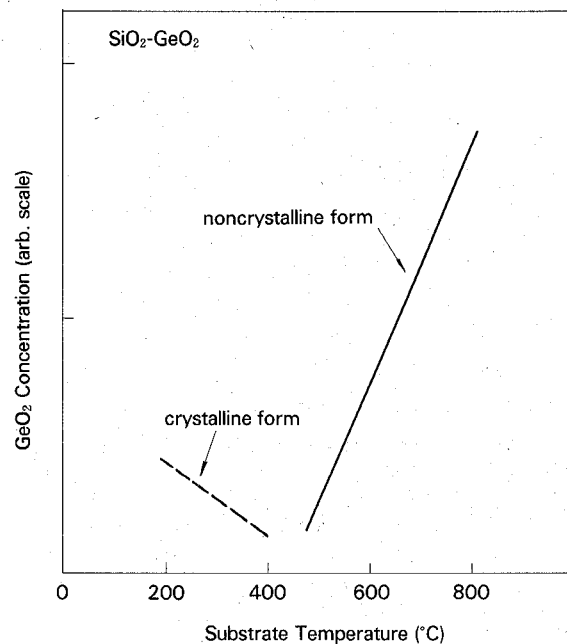


Fig. 6. Substrate temperature dependence of  $\text{GeO}_2$  concentration in the  $\text{SiO}_2$ - $\text{GeO}_2$  system.

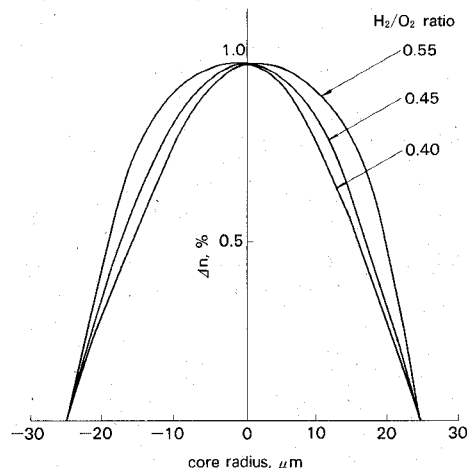


Fig. 7. Relation between the hydrogen/oxygen flow-rate ratio and the refractive index profile of the VAD fibers.

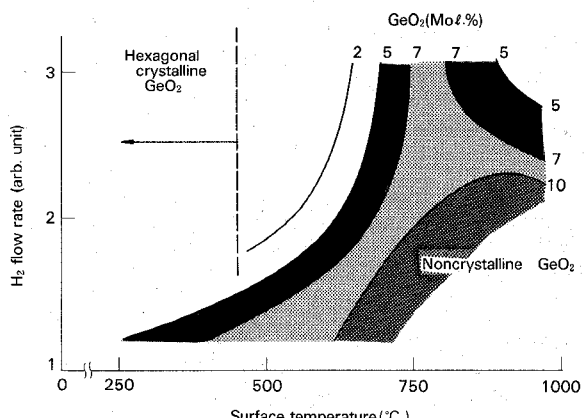


Fig. 8. Porous preform surface temperature dependence of  $\text{GeO}_2$  concentration in  $\text{SiO}_2$  particles.

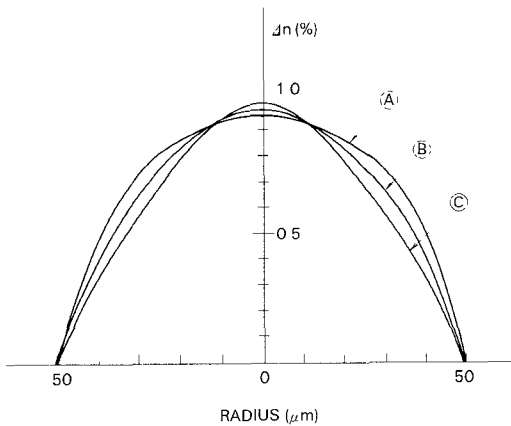


Fig. 9. Refractive index profile with difference  $R$ , where  $R$  is the flow ratio of  $\text{SiCl}_4$  which spouts from the second layer to the mixed gas of  $\text{SiCl}_4$ ,  $\text{GeCl}_4$ , and  $\text{POCl}_3$  which spouts from the center layer. (a)  $R = 0.1$ , (b)  $R = 0.3$ , (c)  $R = 0.5$ , and temperature =  $650^\circ\text{C}$ .

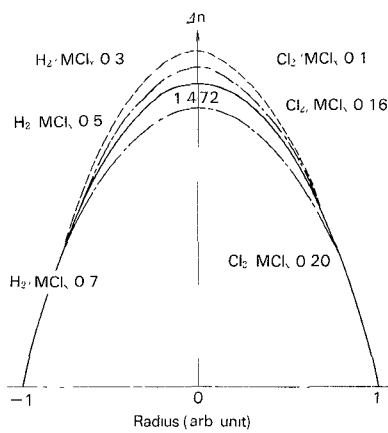


Fig. 10. Change of refractive index profiles against the three different partial pressures of  $\text{H}_2$  and  $\text{Cl}_2$ .

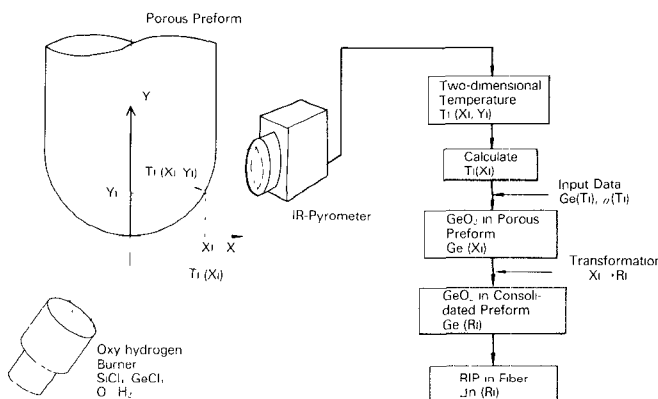


Fig. 11. Computer aided on-line monitoring device on refractive index distribution.  $T_i(X_i, Y_i)$ : temperature,  $Ge(T_i)$ : germanium content at  $T_i$ ,  $\sigma(T_i)$ : soot density at  $T_i$ ,  $R_i$ : radius in fiber, RIP: refractive index profile.

noncrystalline  $\text{GeO}_2$  concentration  $Ge(T_i)$  and soot density  $\sigma(T_i)$  are previously stored as a function of the surface temperature  $T_i$  on the porous preform, the refractive index profile (RIP) can be calculated by measuring surface temperature of the porous preform  $T_i(X_i, Y_i)$ . The accuracy reported was  $\pm 2^\circ\text{C}$  in the temperature measurement from  $400$  to  $800^\circ\text{C}$

with the IR pyrometer, which corresponds to  $\pm 0.05$  mol% in  $\text{GeO}_2$  concentration.

## V. BANDWIDTH CHARACTERISTIC

As far as the refractive index profiles of the VAD fiber are the same as those manufactured by other methods, the bandwidth characteristic will be the same. However, the VAD fiber has a more smooth refractive index profile compared with MCVD and OVPO fibers because the sinusoidal index distortion is small and there is no center dip. Therefore, the VAD method will have a high potentiality to have a wide bandwidth.

Earlier in the development of the VAD method, the bandwidth of the VAD fiber was narrow. As the profile formation mechanisms were made clear, the bandwidth increased year by year. Fig. 12 shows the progress of bandwidth improvement of the VAD fiber [36].

In January 1980, the VAD fiber cable was installed in a field trial of medium/small capacity optical fiber transmission systems in Kawasaki, Japan [3]. Fig. 13 shows the histogram of losses and bandwidths of VAD fibers with the total length of 285 km of fiber [37].

VAD fiber can be sufficiently used for the medium/small capacity optical fiber transmission systems. The large difference between the MCVD fiber and the VAD fiber found in the field trial was the length dependence coefficient  $\gamma$  of bandwidth, where  $\gamma$  is defined by

$$\frac{1}{(\text{BW total})^\gamma} = \sum \frac{1}{(\text{BW individual})^\gamma}.$$

Fig. 14 shows the  $\gamma$  of spliced MCVD and VAD fibers [38]. The  $\gamma$  was distributed from 0.2 to 0.8 in about 2 km. However, the spliced length became 4–5 km;  $\gamma$  approached about 0.5. This large deviation of  $\gamma$  from 0.5 is assumed due to the variation of profile from the optimum  $\alpha$  [38].

Recently, bandwidth characteristics of VAD fibers have been much improved [39], [40] and the maximum bandwidth of 6.7  $\text{GHz} \cdot \text{km}$  was achieved at  $1.3 \mu\text{m}$ , although the length of fiber measured was 4.2 km and the length dependence coefficient  $\gamma$  of 1.0 was used for the calculation [39].

## IV. SINGLE-MODE FIBERS

Single-mode fibers are attractive for a low-loss and wide bandwidth transmission system. The high bit rate, long repeater spacing transmission system requires high reliability fibers, that is, high strength, long length fibers, especially for submarine fiber systems. The VAD technique is quite attractive for the above requirements because of the large size preforms. Continuous 50–100 km single-mode fibers can be drawn from one preform [41]. Moreover, the VAD technique has a high potentiality for the high strength fiber because a VAD preform can be made, if necessary, from all synthesized silica.

The refractive index profile in the VAD fiber has no center dip. Absolute widths of the center dips in MCVD graded index fibers and in MCVD single-mode fibers are almost the same. Therefore, the effect of center dips becomes more important in single-mode fibers because of the small core diameter. The center dip affects the spot size of the fundamental mode. If

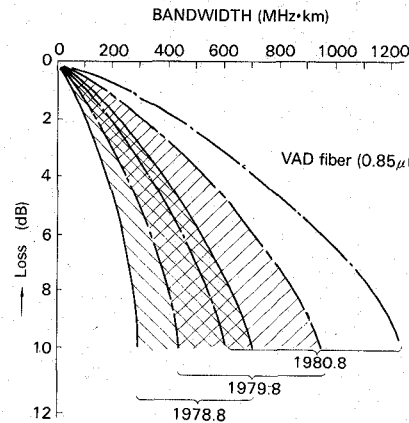
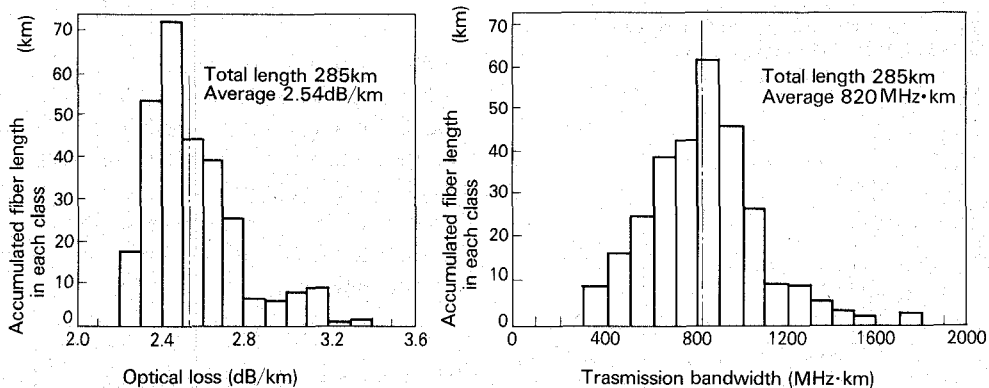
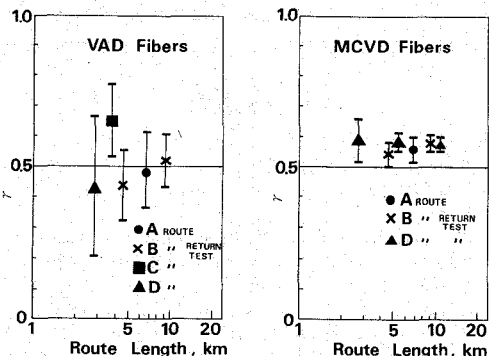
Fig. 12. Improvement of bandwidth of VAD fiber at 0.85  $\mu\text{m}$ .

Fig. 13. Histograms of loss and bandwidth of VAD fibers in the second field trial.

Fig. 14. Distribution of  $\gamma$  of MCVD and VAD fibers in the second field trial.

the center dip is large, the refractive index difference between core and cladding must be large in order to have an effective index difference, that is, the same spot size. This large refractive index difference causes a large Rayleigh scattering loss. This effect becomes especially large for 1.55  $\mu\text{m}$  zero dispersion single-mode fiber because it requires a smaller core and larger NA.

In typical graded index fibers, small content phosphorous is doped in the core in order to reduce the Rayleigh scattering. On the other hand, the merit of usage of phosphorous is small in single-mode fibers because germanium content is initially small in single-mode fibers. Moreover, phosphorous oxide causes loss increase around 1.6  $\mu\text{m}$  due to the absorption of P-OH. The ultra-low loss single-mode fiber was achieved with

a  $\text{SiO}_2\text{-GeO}_2$  core and a  $\text{SiO}_2$  cladding [14]. A 100 km single-mode fiber with a loss of 0.3 dB/km at 1.55  $\mu\text{m}$  was also made with a  $\text{SiO}_2\text{-GeO}_2$  core and a  $\text{SiO}_2$  cladding [41]. There is no report of fluorine dope yet, which is conventionally used in the MCVD method so as to reduce the refractive index of the cladding because the doping of fluorine is considerably difficult in the VAD method.

The most important keys in the production of low-loss single mode fibers are the elimination of core-cladding interface imperfection [45] and the reduction of OH content in the fiber. In order to avoid the core-cladding interface imperfection, core soot and cladding soot must be formed simultaneously by several multiple burners [42].

The consolidation technique and the dehydration technique are almost the same as those for the graded index preform. However, sufficiently thick cladding is required in single-mode fiber in order to prevent the OH contamination from jacketing silica tube.

Fig. 15 shows the relation between OH absorption at 1.24  $\mu\text{m}$  and synthetic cladding diameter/core diameter ratios, which is measured on VAD single-mode fibers [42]. The loss increase at 1.3  $\mu\text{m}$   $\Delta a(1.3)$  has the following experimentally obtained relation with the loss increase due to the OH absorption at 1.24  $\mu\text{m}$ ,  $\Delta a(1.24)$

$$\Delta a(1.3) \approx \frac{1}{3} \times \Delta a(1.24)$$

By this equation, the thickness ratio of the synthetic cladding to core must be more than seven in order to get the loss increase

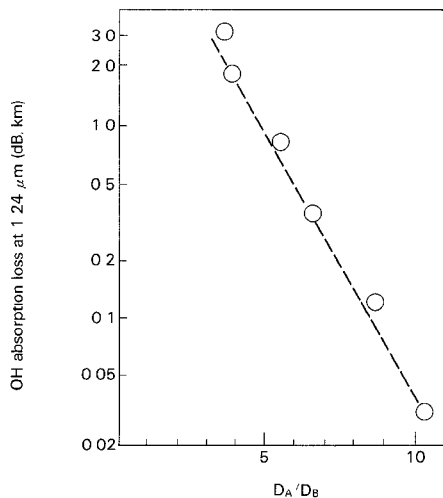


Fig. 15. Relation between OH absorption loss and core cladding diameter ratio.  $D_A$  is the synthetic cladding diameter.  $D_B$  is the core diameter.

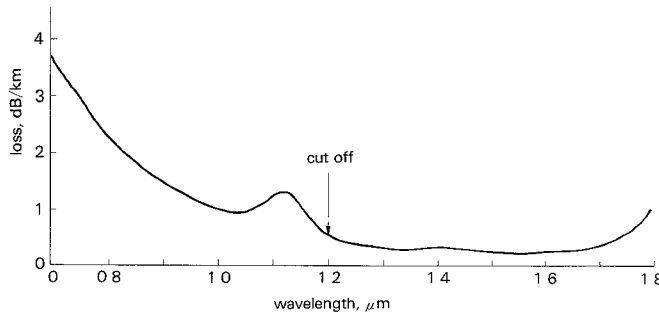


Fig. 16. Loss spectrum of ultra-low loss VAD single-mode fiber.

at 1.3  $\mu\text{m}$  less than 0.1 dB/km. One of the solutions to have a thick cladding is the usage of two burners for the cladding [14]. In this case, oxy-hydrogen gas flow rates between the core and the cladding torches must be carefully balanced in order to have a sufficient cladding thickness.

Fig. 16 shows the measured loss spectrum of a 5 km VAD single-mode fiber characterized by a 125  $\mu\text{m}$  outer diameter, 8.9  $\mu\text{m}$  core diameter, 0.25 percent relative refractive index difference between core and cladding, and a deposited cladding/core diameter ratio of about 7 [14]. The cutoff wavelength of this fiber was about 1.2  $\mu\text{m}$ , the hump around 1.1  $\mu\text{m}$  was attributed to the excess losses of the first higher modes. The losses were 0.35 dB/km at 1.3  $\mu\text{m}$  and 0.2 dB/km at 1.55  $\mu\text{m}$ , respectively.

1.55  $\mu\text{m}$  region zero dispersion single-mode fiber has been made by the VAD method [43]. Fig. 17 shows the refractive index profile of the fiber. The dopant used in the core was germanium only and the cladding was pure silica. The core diameter was 4.2  $\mu\text{m}$  and the refractive index difference was 0.7 percent. The minimum loss obtained at 1.55  $\mu\text{m}$  was 0.32 dB/km, although the loss was somewhat larger than that of the standard single-mode fiber.

## VII. CONCLUSION

In the last two or three years, the fabrication technique by the VAD method has greatly progressed. Ultimately, low OH content graded index fiber and ultra-low loss single-mode fiber have been achieved by the VAD method. The refractive index

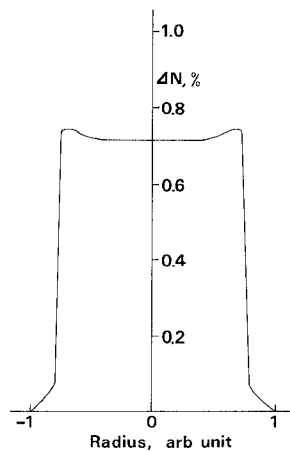


Fig. 17. Refractive index profile of 1.55  $\mu\text{m}$  region zero dispersion VAD single-mode fiber.

profile formation mechanism has been clarified, leading to further improvement. The VAD fiber is now under the mass production stage for the medium/small capacity optical fiber transmission systems. The VAD method is suited for the single-mode fiber because of low OH content and large preform size. In the near future, the VAD single-mode fiber will be used for the high capacity optical fiber transmission systems in both land and under-sea areas.

## ACKNOWLEDGMENT

The author would like to express his appreciation to Dr. N. Niizeki, Dr. H. Takata, and Dr. N. Inagaki of Ibaraki Electrical Communication Laboratory and Dr. S. Shimada and Dr. M. Koyama of Yokosuka Electrical Communication Laboratory, NTT, for their continuous encouragement and suggestions.

## REFERENCES

- [1] T. Izawa, S. Kobayashi, S. Sudo, and F. Hanawa, "Continuous fabrication of high silica fiber preforms," presented at the Int. Conf. on Integrated Optics and Optical Commun., Tokyo, Japan, June 1977.
- [2] T. Izawa and N. Inagaki, "Materials and processes for fiber preform fabrication; Vapor-phase axial deposition," *Proc. IEEE*, vol. 68, pp. 1184-1187, Oct. 1980.
- [3] S. Shimada and N. Uchida, "Field trial of medium/small capacity optical fiber transmission systems," *Elec. Commun. Lab. Tech. J.*, NTT, Japan, vol. 30, no. 9, pp. 2121-2132, 1981.
- [4] T. Moriyama, O. Fukuda, K. Sanada, K. Inada, T. Edahiro, and K. Chida, "Ultimately low OH content V.A.D. optical fibers," *Electron. Lett.*, vol. 16, pp. 698-699, 1980.
- [5] F. Hanawa, S. Sudo, M. Kawachi, and M. Nakahara, "Fabrication of completely OH-free V.A.D. fiber," *Electron. Lett.*, vol. 16, pp. 699-700, 1980.
- [6] N. Inagaki, "Optical fiber fabrication for telecommunication by VAD method," *Nikkei Electron.*, pp. 144-162, Jan. 1981.
- [7] N. Inagaki and T. Edahiro, "Optical fiber fabrication-VAD fiber," in *Optical Devices & Fibers 1982, Japan Annual Reviews in Electronics, Computers & Telecommunications*, Amsterdam, The Netherlands: North-Holland.
- [8] T. Izawa, S. Sudo, F. Hanawa, and T. Edahiro, "Progress in continuous fabrication process of high-silica fiber preforms," in *Proc. 4th ECOC*, Geneva, Switzerland, 1979, pp. 30-36.
- [9] T. Moriyama, O. Fukuda, K. Sanada, K. Inada, S. Tanaka, K. Chida, and T. Edahiro, "Fabrication of ultra-low-OH content optical fibers with VAD method," in *Proc. 6th ECOC*, York, England, 1980, pp. 18-21.
- [10] M. Nakahara, K. Chida, F. Hanawa, S. Sudo, and M. Horiguchi, "Fabrication of low-loss and wide-bandwidth V.A.D. optical fibers at 1.3  $\mu\text{m}$  wavelength," *Electron. Lett.*, vol. 16, pp. 102-103, Jan. 1980.

- [11] N. Shibata, M. Kawachi, S. Sudo, and T. Edahiro, "Low-loss high-numerical-aperture optical fiber fabricated by V.A.D. method," *Electron. Lett.*, vol. 15, pp. 680-681, Oct. 1979.
- [12] S. Sudo, T. Edahiro, and M. Kawachi, "Sintering process of porous preforms made by a VAD method for optical fiber fabrication," *Trans. IECE Japan*, vol. E63, pp. 731-737, Oct. 1980.
- [13] T. Moriyama, R. Yamauchi, K. Sanada, O. Fukuda, S. Chigira, and T. Edahiro, "Reduction of the OH content in the vapour phase axial deposition method by controlling flame hydrolysis reaction," in *Proc. 5th ECOC*, Amsterdam, The Netherlands, 1979, pp. 3.1.1-3.1.4.
- [14] S. Tomaru, M. Yasu, M. Kawachi, and T. Edahiro, "VAD single mode fiber with 0.2 dB/km loss," *Electron. Lett.*, vol. 17, pp. 92-93, 1981.
- [15] S. Tomaru, M. Kawachi, and T. Edahiro, "Fabrication of single mode fibers by VAD," *Electron. Lett.*, vol. 16, pp. 511-512, June 1980.
- [16] S. Sudo, M. Kawachi, T. Edahiro, and K. Chida, "21.2 km graded-index V.A.D. fiber with low-loss and wide bandwidth," *Electron. Lett.*, vol. 16, pp. 152-154, Feb. 1980.
- [17] S. Sudo, H. Okazaki, M. Nakahara, and M. Horiguchi, "Transmission properties of 30.4 km V.A.D. fiber," *Electron. Lett.*, vol. 16, pp. 280-281, Apr. 1980.
- [18] K. Inada, "Optical fiber manufacturing techniques," *J. IECE Japan*, vol. 63, pp. 1150-1156, 1980.
- [19] T. Izawa and S. Sudo, "Continuous fabrication process for high-silica fiber preforms," *Trans. IECE Japan*, vol. E62, pp. 4-10, Nov. 1979.
- [20] M. Nakahara, N. Inagaki, K. Yoshida, M. Yoshida, and O. Fukuda, "Fabrication of a 100 km graded-index fiber from a continuously consolidated VAD preform," in *Tech. Dig. 3rd IOOC*, San Francisco, CA, 1981, paper WD4.
- [21] K. Sanada, T. Shioda, T. Moriyama, K. Inada, S. Takahashi, and M. Kawachi, "PbO doped high silica fiber fabricated by modified VAD," in *Proc. 6th European Conf. on Optical Fiber Commun.*, York, England, 1980, pp. 14-17.
- [22] S. Sudo, M. Kawachi, T. Edahiro, T. Izawa, T. Shioda, and H. Gotoh, "Low-OH-content optical fiber fabricated by vapour-phase-axial-deposition method," *Electron. Lett.*, vol. 14, pp. 534-535, 1978.
- [23] T. Edahiro, M. Kawachi, S. Sudo, and H. Takata, "OH-ion reduction in v.a.d. optical fibers," *Electron. Lett.*, vol. 15, pp. 482-483, Aug. 1979.
- [24] K. Chida, F. Hanawa, M. Nakahara, and N. Inagaki, "Simultaneous dehydration with consolidation for V.A.D. method," *Electron. Lett.*, vol. 15, pp. 835-836, 1979.
- [25] N. Niizeki, "Fabrication of low-loss and long-length optical fibers by VAD," in *Proc. 3rd IOOC*, San Francisco, CA, 1981, paper WD3.
- [26] T. Edahiro, M. Kawachi, S. Sudo, and N. Inagaki, "OH-ion reduction in the optical fibers fabricated by the vapor-phase axial deposition method," *Trans. IECE Japan*, vol. E63, pp. 8-14, Aug. 1980.
- [27] T. Edahiro, K. Chida, Y. Ohmori, and H. Okazaki, "Fabrication technique for graded index optical fibers," in *Rev. Electrical Commun. Lab.*, NTT, vol. 27, pp. 58-68, 1979.
- [28] H. Suda, K. Chida, and M. Nakahara, "Transmission loss in low grade  $\text{SiCl}_4$  V.A.D. fibers," *Electron. Lett.*, vol. 16, pp. 802-803, 1980.
- [29] K. Sanada, T. Moriyama, T. Shioda, O. Fukuda, K. Inada, and K. Chida, "Behavior of  $\text{GeO}_2$  in dehydration process of VAD method," in *Proc. 7th ECOC*, Copenhagen, Denmark, 1981, pp. 2.1.1-2.1.4.
- [30] K. Sanada, T. Shioda, T. Moriyama, K. Inada, M. Kawachi, and H. Takata, "Refractive index profile of the graded index fibers made by V.A.D. method," in *Proc. 5th ECOC*, Amsterdam, The Netherlands, 1979, pp. 5.1.1-5.1.4.
- [31] K. Chida, S. Sudo, M. Nakahara, and N. Inagaki, "On-line monitoring technique of refractive-index-profile in VAD process," in *Conf. Dig. 7th ECOC*, Copenhagen, Denmark, 1981.
- [32] T. Kuwahara, M. Watanabe, S. Suzuki, and S. Sudo, "Refractive index profile formation mechanism on VAD fiber," in *Proc. 7th ECOC*, Copenhagen, Denmark, 1981, pp. 2.2.1-2.2.4.
- [33] M. Kawachi, S. Sudo, N. Shibata, and T. Edahiro, "Deposition properties of  $\text{SiO}_2$ - $\text{GeO}_2$  particles in the flame hydrolysis reaction for optical fiber fabrication," *Japan. J. Appl. Phys.*, vol. 19, pp. L69-L71, 1980.
- [34] T. Edahiro, M. Kawachi, S. Sudo, and S. Tomaru, "Deposition properties of high-silica particles in the flame hydrolysis reaction for optical fiber fabrication," *Japan. J. Appl. Phys.*, vol. 19, pp. 2047-2054, 1980.
- [35] S. Sudo, H. Suda, F. Hanawa, K. Chida, and M. Nakahara, "Refractive index control technique in the vapor phase axial deposition method," in *Proc. Tech. Group IECE Japan*, 1981, paper TGOQE 80-151.
- [36] N. Inagaki, H. Takata, T. Kuroha, M. Hoshikawa, and K. Inada, "Recent progress in optical fiber fabrication technique," in *Proc. Tech. Group IECE Japan*, 1979, paper TGOQE 79-70.
- [37] Y. Ishida, Y. Katsuyama, S. Seikai, C. Tanaka, and Y. Mitsunaga, "Design and characteristics of graded-index optical cables for use in *Elec. Commun. Lab. Tech. J.*, vol. 30, pp. 2167-2180, 1981.
- [38] T. Tanifugi, T. Horiguchi, M. Nakahira, K. Omote, and M. Tokuda, "Loss and baseband frequency response of transmission lines in the field trial of medium/small capacity optical fiber transmission systems," in *Elec. Commun. Lab. Tech. J.*, NTT, Japan, vol. 30, pp. 2193-2204, 1981.
- [39] M. Nakahara, S. Sudo, N. Inagaki, K. Yoshida, S. Shibuya, K. Kokura, and T. Kuroha, "Ultra wide bandwidth V.A.D. fiber," *Electron. Lett.*, vol. 16, pp. 391-392, May 1980.
- [40] T. Edahiro, M. Kawachi, and S. Sudo, "Transmission characteristics of 116.3 km and 65.1 km graded index V.A.D. fibers at 1.55  $\mu\text{m}$  and 1.3  $\mu\text{m}$ ," *Electron. Lett.*, vol. 16, pp. 477-478, June 1980.
- [41] M. Kawachi, S. Tomaru, M. Yasu, M. Horiguchi, S. Sakaguchi, and T. Kimura, "100 km single mode VAD fibers," *Electron. Lett.*, vol. 17, pp. 57-58, 1981.
- [42] T. Miya, M. Nakahara, N. Yoshioka, M. Watanabe, Y. Furui, and O. Fukuda, "Transmission characteristics of VAD single-mode fiber," in *Proc. 7th ECOC*, Copenhagen, Denmark, 1981, post deadline paper, pp. 22-25.
- [43] T. Moriyama, M. Miyamoto, M. Akiyama, O. Fukuda, T. Miya, and K. Chida, "Fabrication of low loss and long length VAD fibers for 1.55  $\mu\text{m}$  wavelength region," in *Proc. 8th ECOC*, Cannes, France, Sept. 1982, paper A II-1.
- [44] M. Miyamoto, R. Yamauchi, K. Inada, and T. Tanifugi, "Length dependence of bandwidth for fibers with small axial profile fluctuations," in *Proc. IOOC '81*, San Francisco, CA, 1981, paper WG3.
- [45] K. Inada, R. Yamauchi, and M. Miyamoto, "Wavelength dependence of geometrical imperfection losses in single mode fibers," in *Proc. 8th ECOC*, Cannes, France, Sept. 1982, paper C19.



Koichi Inada (M'73) was born in Tochigi, Japan, on February 24, 1941. He received the Ph.D. degree from the Tokyo Institute of Technology, Tokyo, Japan, in 1976.

In 1963 he joined Fujikura Cable Works, Ltd., Chiba-ken, Japan, where he is currently head of the Optical Fiber and Cable Development Division. He has been engaged in research and development of high frequency coaxial cables, super conducting cables, millimeter waveguide, and optical fibers.

Dr. Inada is a member of the Institute of Electronics and Communication Engineers of Japan.